APPLICATION OF LASER DOPPLER VELOCIMETRY (LDV) TO STUDY THE STRUCTURE OF GRAVITY CURRENTS UNDER FIRE CONDITIONS

B Moghtaderi[†]
Process Safety and Environment Protection Group
Discipline of Chemical Engineering, School of Engineering
Faculty of Engineering & Built Environment, The University of Newcastle
Callaghan, NSW 2308, Australia

ABSTRACT

Gravity currents are of considerable safety importance primarily because of their role in the spread and transport of smoke and hot gases in building fires. Despite recent progress in the field, relatively little is known about the structure of gravity currents under conditions pertinent to building fires. The present investigation is an attempt to address this shortcoming by studying the turbulent structure of gravity currents. For this purpose, a series of experiments was conducted in a rectangular tank with turbulent, sub-critical underflows. Laser-Doppler Velocimetry was employed to quantify the velocity field and associated turbulent flow parameters. Experimental results indicated that the mean flow within the head region primarily consisted of an undiluted large single vortex which rapidly mixed with the ambient flow in the wake region. Cases with isothermal wall boundary conditions showed three-dimensional effects whereas those with adiabatic walls exhibited two-dimensional behaviour. Turbulence was found to be highly heterogeneous and its distribution was governed by the location of large eddies. While all components of turbulence kinetic energy showed minima in the regions where velocity was maximum (i.e. low fluid shear), they reached their maximum in the shear layer at the upper boundary of the flow.

KEY WORDS: gravity currents, laser Doppler velocimetry, turbulent structure

INTRODUCTION

Gravity currents are important physical phenomena which have direct implications in a wide variety of physical situations ranging from environmental phenomena[‡] to enclosure fires. Gravity currents have been extensively studied in the geophysical science and Kneller & Buckee [1] provide an excellent review of these studies (over 150 papers). Gravity currents are also of great importance in fire safety research because they are responsible for the spread of smoke, toxic materials and hot gases generated by fires within buildings [2-8].

A gravity current (GC) is the flow of one fluid into another caused by a difference in density. The density difference, in turn, may be due to a dissolved chemical or temperature difference between the two fluids [5,8]. Gravity currents are usually formed when either a lighter fluid is introduced at the top of a heavier ambient fluid or a more

[†] Corresponding author, Ph: +61 (2) 4921-6920, Fax: +61 (2) 4921-6920, Email: cgbm@cc.newcastle.edu.au
[‡] Common examples include: sea breeze fronts, avalanches, and flows following volcanic eruptions.

dense fluid is issued at the bottom of an ambient fluid [7]. The anatomy of a gravity current [9-12] shows a head region at its leading portion where significant mixing occurs followed by a laminar flow of the GC fluid. There are two forms for the GC head, namely: (a) billows, and (b) lobes and clefs. Billows are primarily two-dimensional (2D) structures, whereas lobes and clefs are essentially three-dimensional (3D) patterns formed when a source of instability (e.g. heat transfer) is introduced into the gravity current.

Meaningful modelling of gravity currents and interpretation of their characteristics requires detailed knowledge of the velocity and turbulent structure within such flows [7]. While a reasonable amount of data is now available on the behaviour of gravity currents under conditions pertinent to building fires (particularly under adiabatic conditions), relatively little work has been undertaken on their turbulent structure [5].

The present work is part of a larger project which attempts to address this deficiency by: (1) obtaining detailed information on the turbulent flow field within gravity currents, and (2) gaining insight into the turbulent energy distribution in terms of eddy frequency and size. The ultimate goal of this research is to further improve our understanding of gravity currents and, thereby, enhance the capabilities of the existing mathematical models for predicting the transport of smoke and hot gases in building fires. The results presented in this paper were obtained under both adiabatic and isothermal wall boundary conditions using Laser Doppler Velocimetry (LDV) technique. The current measurements are different from earlier works [11-12] in a sense that they were obtained under two different heat transfer conditions in order to investigate the impact of heat transfer on the structure of the gravity currents.

EXPERIMENTAL

The Scaled Physical Model

Experiments were conducted in a scaled physical model consisting of a 2.2-m-long, 0.2-m-wide, and 0.2-m-deep rectangular Perspex tank fitted with a 0.3-m-long lock compartment at one end and a cooling jacket at the bottom surface (Figure 1). The cooling system was employed to generate temperatures well below the fluid temperature and, thereby, simulate the heat losses associated with the isothermal wall boundary condition at the bottom surface. For adiabatic experiments, the tank was insulated with 25 mm polystyrene foam on all surfaces and the cooling system was turned off.

While the tank was filled with the ambient fluid (988 kg/m^3), the lock compartment contained a salt solution of density 1035 kg/m^3, representing the denser fluid. The temperature of both fluids were kept approximately at 19 ^{0}C.

The scaling was carried out on the basis of "Froude Scale Modelling" approach in which the currents were fully characterised by dimensionless variables such as Froude number (Fr), the normalised density difference $g^{/}$, and the scaled characteristic height (h^*):

$$Fr = V^* / \sqrt{g'gH} \tag{1}$$

$$g' = \left(\rho_d - \rho_a\right) / \rho_a \tag{2}$$

$$h^* = d / H \tag{3}$$

where V^*, H, g, ρ_d, ρ_a, and d are the characteristic velocity, the total fluid depth, the gravitational acceleration, the dense fluid density, the ambient fluid density, and the mean gravity current thickness, respectively.

Table 1 provides a summary of the flow parameters of gravity currents generated in this study. Results for the scaled characteristic height and Fr number relevant to both adiabatic and isothermal (i.e. heat loss) boundary conditions have been summarised in this table. The literature (and indeed out own results) suggests [5] that the Fr is independent of g' and depends only on the geometry of the system. Since the tank and the lock compartment were both filled to a depth of 0.12 m, the salt-water tank set-up represents a 1/20 scale model of typical dwellings having room heights of 2.4 m. It should be mentioned that because of independence of the Fr from g', the results of this study are expected to apply directly to actual gravity currents generated in typical building fires. For instance, for a head velocity of 0.1 at a $g' = 0.048$ under adiabatic conditions the Fr number of the salt-water tank set-up is 0.59. This would correspond to a velocity of 2.18 m/s at a $g' = 0.58$[‡] in a 2.4 m high dwelling.

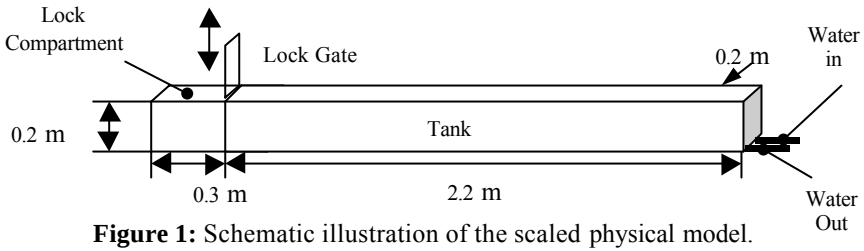

Figure 1: Schematic illustration of the scaled physical model.

Table 1: Summary of flow parameters.

Parameter	Value	
	Adiabatic	Isothermal
Ambient fluid density (ρ_a)	988 kg/m^3	988 kg/m^3
Dense fluid density (ρ_d)	1035 kg/m^3	1035 kg/m^3
Ambient fluid viscosity (μ_a)	1.62×10^{-3} (NS)/m^2	1.62×10^{-3} (NS)/m^2
Dense fluid viscosity (μ_d)	1.14×10^{-3} (N S)/m^2	1.14×10^{-3} (N S)/m^2
$g' = (\rho_d - \rho_a)/\rho_a$	0.048	0.048
Mean gravity current thickness (d)	0.06 m	0.06 m
Total fluid depth (H)	0.12 m	0.12 m
Head velocity* (u_h) at x = 0.8 m	0.1 m/s	0.079 m/s
Maximum mean temporal velocity in X direction (u_{max})	0.15 m/s	0.122 m/s
Average velocity over the entire depth (u_{mean})	0.07 m/s	0.055 m/s

[‡] This value represents the density difference between the ambient and hot air at 298 and 473 K, respectively.

Reynolds number based on u_h, $Re = (\rho_d u_h d)/\mu_d$	5.5×10^3	4.35×10^3
Reynolds number based on u_{mean}, $Re = (\rho_d u_{mean} d)/\mu_d$	3.8×10^3	2.99×10^3
Froude number based on u_h, $Fr = (u_h)/\sqrt{g'gd}$	0.59	0.466
Froude number based on u_{mean}, $Fr = (u_{mean})/\sqrt{g'gd}$	0.42	0.33
Richardson number based on u_h, $Ri = (g'gd)/u_h^2$	2.82	1.76
Richardson number based on u_{mean}, $Ri = (g'gd)/u_{mean}^2$	5.74	3.54

* Calculated from both video records and LDV analysis.

Laser Doppler Velocimetry

Laser Doppler Velocimetry (LDV) is a well-proven non-intrusive technique that accurately measures the mean and fluctuating components of fluid velocity and, thereby, allows us to calculate turbulent parameters, such as turbulent kinetic energy, turbulent production rates and Reynolds stresses. In this technique a single laser beam is split into two equal-intensity beams focused at a common point (measuring volume) in the flow field. Particles moving through this point scatter the laser light, some of which is collected by a photodetector. The output frequency of the photodetector is directly related to the flow velocity. If additional pairs of laser beam with different wavelengths are directed at the same point, two or even three velocity components can be simultaneously determined. To enhance the quality of signals it is often desirable to seed the flow with suitable particles.

It should be noted that LDV provides point measurements of velocity components. If one uses a traverse system to move the laser light source, it would be possible to perform an area analysis by combing the point-by-point measurements.

In this study instantaneous velocity components were measured using a three-component (3D) LDV system operated with a 2W water-cooled argon-ion laser. The system was equipped with a 83 mm diameter fibre-optic probe having a 180-mm focal distance. The probe included both focusing and receiving optics in one compact unit. The measurement volume was located at different distances from the tank side-wall (see below). The dimensions of the measuring volume in vertical, downstream, and cross-stream directions were 0.08 mm, 0.08 mm and 1 mm for the horizontal velocity component (u) and 0.08 mm, 0.08 mm, and 0.9 mm for the vertical (v) and cross-stream (w) velocity components, respectively. Polystyrene Latex (PSL) particles suspended in a dilute solution were added to both ambient and dense fluids using a TSI single-jet atomiser to improve the signals. The signal quality was further enhanced by matching the refractory indices of the two fluids and, hence, minimising the refraction of the laser beams due to mixing between the two fluids. This was achieved by using a mixture of water and propane-2-ol with a density of 988 kg/m^3 as the ambient fluid (see references [11-12] for more details).

A three-dimensional picture of the velocity field was constructed from a succession of identical experiments with the fibre-optic probe positioned differently for each using a high-precision traverse system. Sixty velocity profiles were constructed by measuring the

velocity components at six stations along the axial axis (0.5, 0.6, 0.7, 0.8, 0.9, and 1 m away from the lock gate) and ten equally spaced stations along cross-stream axis (0.01-0.1 m away from the side wall). Each profile consisted of twenty measurement points above the bottom of the tank at heights 1, 2, 3, 4, 5, 8, 11, 14, 17, 20, 25, 30, 35, 40, 45, 50, 60, 70, 90, 110 mm.

RESULTS AND DISCUSSION

General Characteristics of the Mean Flow

In order to construct the necessary velocity profiles, it was necessary to perform almost identical experiments with flow parameters (e.g. Reynolds, Froude and Richardson numbers) relevant to gravity currents in typical building fires. As shown in Table 1, the general characteristics of the underflows observed in this study were similar to those reported by others [1-11]. In particular, we observed how the ambient fluid, bounced back by the tank end wall, affected the head of the gravity current. The impact, however, was limited to regions in the vicinity of the lock gate. Within the area of interest (0.5 m to 1 m away from the lock gate) the head velocity was constant and the flow field remained quasi-steady for several seconds after the current had passed through. For the adiabatic case, the head velocity of the current within the measured section was 0.1 m/s with a corresponding dimensionless value of 0.42 which is consistent with the values reported in the literature [12,13].

The schematic of a typical underflow generated in this study is shown in Figure 2. As can be seen the gravity current comprises of two main sections: head, and body. The flow in each section consists of an inner and an outer region. The maximum temporal mean velocity in x direction (u_{max}) occurs at the interface between these two regions. To identify the upper boundary of the gravity current (i.e. the interface between the ambient and dense fluids), in a number of selected experiments potassium permanganate was added to the dense fluid to improve visualisation. Typically, u_{max} was found to occur at a height equivalent to 20% of the flow thickness (d). A high velocity core that supplies fluid to the head is centred around this region. While the height at which u_{max} occurs varies slightly with downstream distance, its value decreases with the distance from the head.

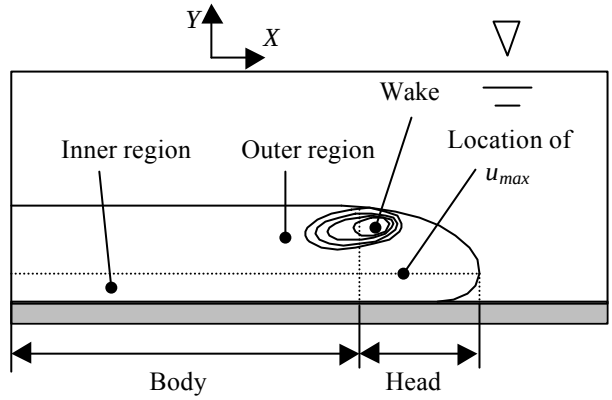

Figure 2: Schematic of a typical flow.

Typical vector maps of the temporal mean velocity in x direction (u) are shown in Figure 3 for both adiabatic and isothermal wall boundary conditions. These particular maps were constructed from the detailed profiles at x = 0.8 m (adiabatic case) and x = 0.6 m (isothermal case) by transforming successive 80-ms time frames into the spatial domain

utilising the head velocity. A Lagrangian reference frame, fixed to the moving head, was used in transformation of the data into the spatial co-ordinate system. Figure 3 clearly illustrates the excess velocity of fluid entering the head, the flow pattern in the ambient fluid, and the general circulation of the fluid within the head region due to the upward movement of the fluid supplied to the head. As can be seen, there is a great deal of similarities between gravity current formed under isothermal and adiabatic wall boundary conditions. In particular, the vertical profile of u, when normalised against u_{max}, is almost identical in both cases (see Figure 4). Despite similarities, the speed of the head velocity for the isothermal case (where there is significant heat loss from the bottom of the tank) is almost 21% less than that of the adiabatic boundary condition (compare the position of the nose in Figures 3a and 3b). This is primarily due to the fact that the intense mixing in the head region greatly facilitates the heat transfer process and, thereby, causes the formation of longitudinal rolls. These three-dimensional structures, in turn, slow down the gravity current and enhance the heat transfer process. Figure 5 illustrates the vector map of the gravity current in a cross-stream plane at an axial station of x = 0.8 m. Both adiabatic and isothermal wall boundary conditions show some three-dimensional structure, however, the latter exhibits larger and much more intense 3D behaviour. It should be noted that our experimental results showed symmetrical flow patterns in the cross-stream direction. For this reason only half of the flow domain has been plotted in Figure 5.

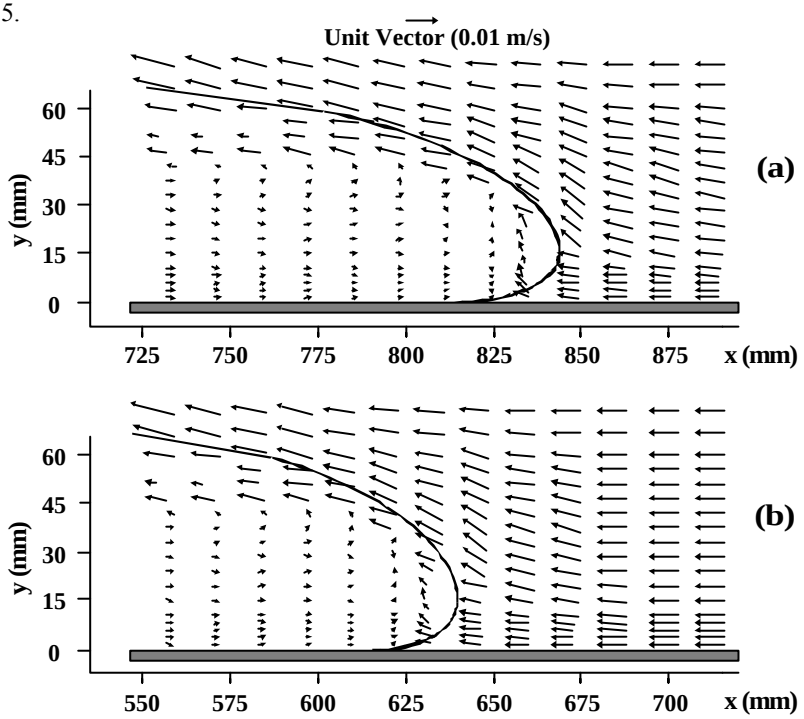

Figure 3: Vector maps of mean temporal velocity within the head region in a x-y plane under (a) adiabatic boundary condition and (b) isothermal wall boundary condition in which the bottom temperature is kept at a temperature below the fluid temperatures.

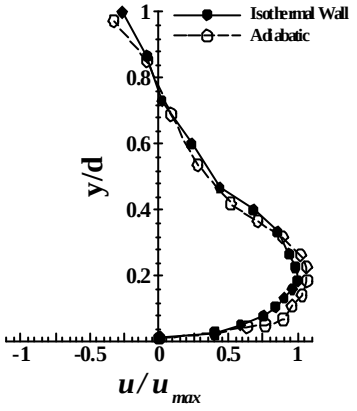

Figure 4: Vertical profiles of the axial component of the mean temporal velocity at x = 0.8 m for adiabatic and isothermal wall boundary conditions. The velocities and heights were normalised against u_{max} and gravity current thickness (d), respectively.

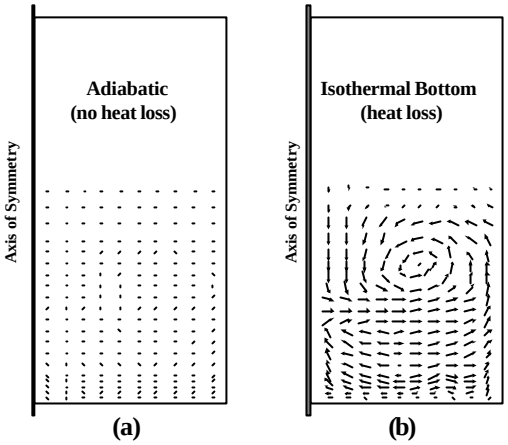

Figure 5: Vector maps of mean temporal velocity in a y-z (cross-stream) plane at an axial station of x = 0.8 m under: (a) adiabatic boundary condition and (b) isothermal wall boundary condition. Note that due to symmetry only half of the flow domain has been shown.

Turbulent Flow Structure

Components of turbulent velocity (u', v', and w') were calculated from the root-mean squares of the fluctuating components of the velocities (u_f, v_f, and w_f) taken over 100-ms timeframes. Fluctuating components were obtained by subtracting the instantaneous components of velocity (u_i, v_i, and w_i) from their corresponding temporal mean velocities (u, v, and w). Figure 6 illustrates the temporal variations of axial (u'), vertical (v') and cross-stream (w') turbulent velocity components for a typical point (x = 0.8, y = 0.02, z = 0.02) within the flow domain under isothermal wall boundary conditions. The peaks in Figure 6 are associated with the passage of the gravity current head and relatively large turbulence

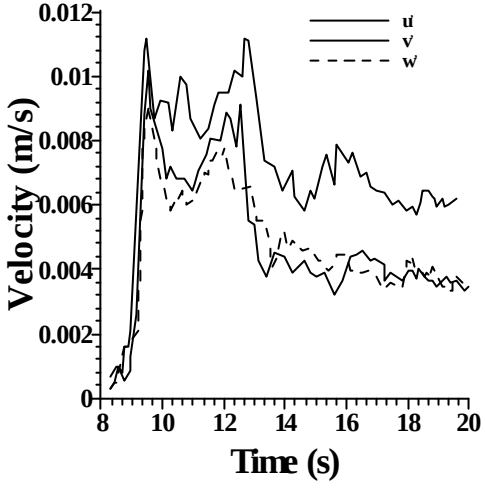

Figure 6: Three-dimensional components of turbulent velocity under isothermal conditions at x = 0.8, y = 0.02, z = 0.02.

eddies. Interestingly, under isothermal wall boundary conditions where the extent of heat losses is significant, v' and w' are of the same order of magnitude and they are both in phase with u'.

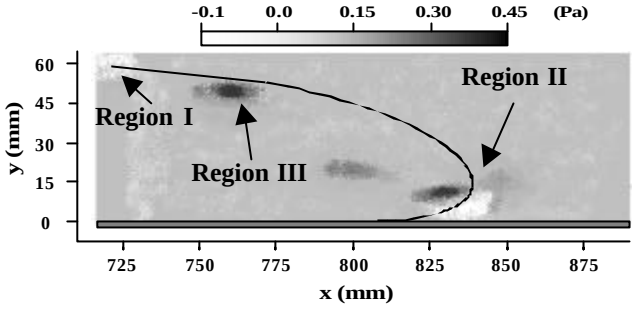

Figure 7: Grey-scaled map of Reynolds stress within the head region in a x-y plane (z=0.02). This map was constructed from the turbulent velocity components obtained under adiabatic boundary conditions.

Calculations show that the highest turbulent velocities occur along the interface between the gravity current and the ambient fluid, particularly, at the nose region. The distribution of Reynolds stresses (e.g. τ_{xy}[†] in x-y plane) within the current exhibits the same trend (see Figure 7). As can be seen, there are three regions of high magnitu-de Reynolds stress. One with an overall negative value lies within the shear layer behind the head (left hand top corner in Figure 7). This is related to the transfer of momentum from the dense fluid (i.e. fluid in the gravity current) into the ambient fluid due to the formation of the wake behind the head. The second region of high Reynolds stress, with both positive and negative values, is in the vicinity of the nose. The formation of this high Reynolds stress region can be partly attributed to the upward flow of the ambient fluid into the gravity current head and formation of vortical structures. The third high Reynolds stress region, located at the edge of the wake, is perhaps related to the upward and backward flow of the ambient fluid into the dense fluid as it is incorporated into the wake.

The total kinetic energy, k, for both adiabatic and isothermal boundary conditions was calculated from equation (1) using three-dimensional components of the turbulent velocity:

$$k = 0.5 \times (\overline{u'^2} + \overline{v'^2} + \overline{w'^2}) \qquad (4)$$

Typical results for an isothermal case are shown in Figure 8 where profiles of the axial, vertical and cross-stream components of the turbulent kinetic energy have been plotted against the dimensionless height (y/d). The axial and cross-stream co-ordinates of all data points shown in Figure 8 are x = 0.8 and z = 0.02, respectively.

All three components of the turbulent kinetic energy reach a minimum around y/d = 0.2 that approximately coincides with the height at which velocity is maximum and shear stress is minimum. To examine the relative importance of small and large turbulent eddies, the axial component of the turbulent kinetic energy, shown in Figure 8, was partitioned into two profiles on the basis of turbulent frequency. The results have been summarised in Figure 9 where the profile associated with frequencies greater than 10 Hz

[†] Calculated from: $\tau_{xy} = -\rho_d \overline{u'v'}$.

represents small eddies while the profile related to frequencies smaller than 10Hz represents large eddies[†]. As Figure 9 illustrates, the axial component of the turbulent kinetic energy is dominated by low frequencies indicating that most of the turbulent energy is contained within large eddies[‡]. Assuming that eddies are transported by the mean flow, the dominant turbulent length scale is about 0.01 m. This value is comparable with the value of 0.03 m reported by Kneller [12] for lock exchange currents.

The energy content of small eddies are evidently much less than large eddies (Figure 9). In addition, the energy distribution within the small eddies (fr > 10 Hz) varies little with height in the flow. However, there is a systematic increase in the turbulent energy associated with small eddies for dimensionless heights of up to 0.15, highlighting the importance of shear in the formation of small eddies within the inner region.

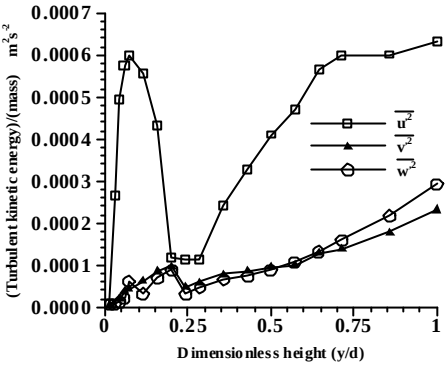

Figure 8: Axial, vertical and cross-stream components of the turbulent kinetic energy as a function of dimensionless height. Note that the height has been normalised against the depth of the gravity current.

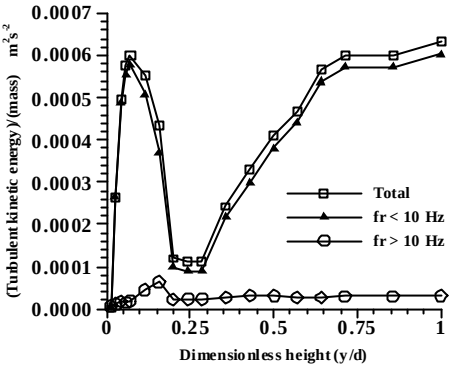

Figure 9: Components of the axial (horizontal) turbulent kinetic energy as a function of dimensionless height. Note that the total energy has been partitioned on the basis of a frequency of 10 Hz.

CONCLUSIONS

Turbulent flow structures of gravity currents were studied under adiabatic and isothermal wall boundary conditions using Laser Doppler Velocimetry (LDV) techniques. Regardless of the boundary conditions, the currents consisted of a head attached to a body. Both of these elements comprised of an inner and outer layers. Experimental results indicate that the gravity currents formed under adiabatic boundary conditions have essentially a two-dimensional structure whereas currents associated with isothermal wall boundary conditions exhibit three-dimensional behaviour, primarily, due to the formation

[†] The profile for $\overline{u'^2}\Big|_{fr>10}$ was calculated from 100-ms time averages whereas the other profile ($\overline{u'^2}\Big|_{fr<10}$) was obtained from the difference between the former and the total.

[‡] The same trends were observed for vertical and cross-stream components of the turbulent kinetic energy.

of longitudinal rolls. As such, currents formed under adiabatic conditions propagate with velocities higher than those associated with currents generated under isothermal wall boundary conditions. A study of Reynolds stresses reveals that large negative shear stresses occur in the wake region behind the head where ambient fluid is drawn in to the current. Analysis of turbulent kinetic energy shows that minimum levels of turbulence are reached in the regions where velocity is maximum and, thereby, shear stress is low. In addition, large eddies appear to dominate the flow. The characteristic length (length scale) of such eddies is estimated to be comparable with the thickness of the dense underflow.

ACKNOWLEDGEMENTS

The author would like to acknowledge the financial and in-kind supports provided to him by the Universities of Newcastle and Adelaide.

REFERENCES

1. Kneller, B.C., and Buckee, C., "The Structure and Fluid Mechanics of Turbidity Currents: A Review of Some Recent Studies and Their Geological Implications", *Sedimentology*, **47** (Suppl 1), pp 62-94, 2000.
2. Stekler, K.D., Baum, H.R., and Quintere, J.G., "Salt Water Modelling of Fire Induced Flows in Multi-Component Enclosures", *21st Symposium (Int.) on Combustion*, pp 143-149, 1986.
3. Chobotov, M., Zukoski, E.E., and Kubota, T., "Gravity Currents with Heat Transfer", NBS-GCR-87-522, 1987.
4. Pagni, P.J., and Fleischmann, C.M., "Backdraft Phenomena", NIST-GCR-94-646, 1994.
5. Fleischmann, C.M., Pagni, P.J., and Williamson, R.B., "Salt Water Modelling of Fire Compartment Gravity Currents", *Proceedings of the Forth International Symposium on Fire Safety Science*, Canada, pp 253-264, 1994.
6. Baum, H.R., Cassel, K.W., McGrattan, K.B., and Rehm, R.G., "Gravity Current Transport in Building Fires", *Int. Conf. on Fire Research and Engineering*, Orlando FL, USA, pp 27-32, 1995.
7. Rehm, R.G., McGrattan, K.B., Baum, H.R., and Cassel, K.W., "Transport by Gravity Currents in Building Fires", *Proceedings of the Fifth International Symposium on Fire Safety Science*, Australia, pp 391-402, 1997.
8. Fleischmann, C.M., and McGrattan, K.B., "Numerical and Experimental Gravity Currents Related to Backdrafts", *Fire Safety Journal*, **33** (1), pp 21-34, 1999.
9. Benjamin, T.B., "Gravity Currents and Related Phenomena", *J. Fluid Mechanics*, **31**, pp 209-248, 1968.
10. Simpson, J.E., "*Gravity Currents in the Environment and the Laboratory*", Halsted Press, New York, 1987.

11. Kneller, B.C., Bennett, S.J., and McCaffrey, W.D., "Velocity and Turbulence Structure of Density Currents and Internal Solitary Waves: Potential Sediment Transport and the Formation of Wave Ripples in Deep Water", *Sediment. Geol.*, **112**, pp 235-250, 1997.

12. Kneller, B.C., Bennett, S.J., and McCaffrey, W.D., "Velocity Structure, Turbulence and Fluid Stresses in Experimental Gravity Currents", *J Geophysical Res.*, 104, pp 5381-5391, 1999.

13. Middleton, G.V., "Experiments on Density and Turbidity Currents, I, Motion of the Head", *Canadian J. Earth Sci.*, **3**, pp 523-546, 1966.